18èmes Journées Internationales de Thermique (JITH 2017)
Monastir (Tunisie), 25 - 27 Octobre 2017

Unstructured control volume-lattice Boltzmann method for solving unsteady conduction heat transfer

F[1]. Bouzgarrou, F[1, 2]. Askri, S[1]. Ben Nasrallah
[1]Laboratory of Energy and Thermal Systems (LESTE), Engineering School of Monastir, University of Monastir, 5000 Monastir, Tunisia
[2]Engineering Faculty, King Khalid University, Abha, Saudi Arabia

bouzgarroufatma@yahoo.fr
faouzi.askri@yahoo.fr
sassi.bennasrallah@yahoo.fr

Abstract :

In this paper a numerical approach is presented by the authors for the prediction of unsteady conduction heat transfer problem in a complex two-dimensional geometry using a general unstructured grid. This approach is based on the Control Volume finite element scheme and the Lattice Boltzmann Method (CVLBM for short) and the use, for the first time, of the Skew Positive Coefficient Upwind scheme (SPCU**)** and the matrix formulation of the discretized Lattice Boltzmann Equation (LBE). To examine its accuracy and computational efficiency, three test cases (a square enclosure, an equilateral triangular enclosure and a quarter of a circle with a rectangular enclosure) are investigated and are also solved using the conventional Control Volume Finite Element Method (CVFEM). In all the cases, the CVLBM was found to provide accurate results. In addition, a new time-discretization scheme was proposed and the computer procedure based on this numerical scheme needs an accurate CPU time and is stable in treating unsteady conduction heat transfer within complex geometry.

Keywords :

Boltzmann equation, Lattice Boltzmann method, CVFEM, conduction heat transfer.

1. Introduction

In the two last decades, the Lattice Boltzmann Method (LBM) has undergone a major progress as a powerful technique for computing fluid flow and heat transfer problems.

The LBM is based on the kinetic theory in which it studies the particle interactions by using the particle mass distribution function. This mechanism is parallel in nature due to the locality of the dynamic of particles. From a computational point of view, it is well suitable for massively parallel computing. Simplicity of programming and ease of considering microscopic interactions for modeling of additional physical phenomenon are the other advantages of the LBM [1].

However, uniform and regular spatial lattices represent a severe limitation for many practical engineering purposes including real-life complex geometries especially when there is a need for high resolutions near the body or the walls such as cars and air planes.

Therefore, in the recent years, some efforts have been made in literature to apply the traditional numerical methods developed in computational fluid dynamics (CFD) for solving the discrete Boltzmann equation (DBE). Finite-difference (FD) [2–7], finite-volume (FV) [8–14], finite-element (FE) [15], and recently spectral-element discontinuous Galerkin (SEDG) [16–17] methods have been applied in order to improve the computational accuracy and efficiency of the LBM.

All these works are interested to fluid flow problems. For heat transfer problems, few works have been done. Mishra el al. [18] have used the LBM to solve the unsteady heat conduction problems in 1-D, 2-D and 3-D

Cartesian geometries with uniform and non-uniform lattices and it was compared with the finite difference method (FDM).

Mondal and Li [19] have studied the natural convection in the presence of volumetric radiation in a square cavity containing an absorbing, emitting and scattering medium using the LBM with non-uniform lattices/ control volumes. All results were compared with the results with uniform lattices/control volumes and were found to provide accurate results. In all the cases investigated, the method of non-uniform lattices is more computationally efficient compared to the solution with uniform lattices.

Z.Xi Tong et al. [20] have studied the efficiency of the coupling method between the Lattice Boltzmann Method (LBM) and the Finite Volume Method (FVM) for the multiscale multi-component diffusion processes.

To the author's best knowledge, no works on the BGK-Boltzmann equation in conjunction with the unstructured control volume technique for solving heat transfer problems in complex geometries have been done. So, the main objective of this paper is to implement the unstructured Control Volume- Lattice Boltzmann Method (CVLBM) for solving unsteady conduction heat transfer problems within any arbitrary 2-D geometry.

The paper is organized as follows. The discrete LBE is presented at first. Then, the theoretical background of the CVLBM and the matrix formulation of the Discretized LBE are presented. The last section is devoted to present the numerical results for unsteady conduction heat transfer to examine the accuracy and performance of the solution of the CVLBM implemented in unstructured mesh.

2. Boltzmann equation

In the absence of convection, radiation and heat generation, the energy equation is given by

$$\rho C_p \frac{\partial T}{\partial t} + \vec{\nabla}.\left(-\lambda \vec{\nabla} T\right) = 0 \quad (1)$$

Where ρ is the density, C_p is the specific heat and λ is the thermal conductivity.

The Boltzmann equation with the single relaxation time approximation, the so-called Bhatnagar-Gross-Krook (BGK) model, is given by

$$\frac{\partial f_i}{\partial t} + \vec{c}_i.\nabla f_i = \frac{f_i^{eq} - f_i}{\tau},\ i = 0...n_v \quad (2)$$

Where n_v is the number of different discrete velocities in the model, f_i^{eq} is the particle equilibrium distribution function (the Maxwell-Boltzmann distribution function) associated with motion along the i^{th} direction in velocity space $\vec{c}_i$, and τ is the relaxation time.

In the present work, the relaxation time τ, the nine velocities $\vec{c}_i$ and their corresponding weights of the D_2Q_9 lattice [21] are the following:

$$\tau = \frac{3\alpha}{c^2} + \frac{\Delta t}{2} \quad (3)$$

$$\vec{c}_i = \begin{cases} (0,0),\ i = 0 \\ c\left[cos\left((i-1)\frac{\pi}{4}\right), sin\left((i-1)\frac{\pi}{4}\right)\right],\ i = 1...4 \\ \sqrt{2}c\left[cos\left((i-1)\frac{\pi}{4}\right), sin\left((i-1)\frac{\pi}{4}\right)\right],\ i = 5...8 \end{cases} \quad (4)$$

$$\omega_i = \begin{cases} \frac{1}{9} & for \quad i = 0 \\ \frac{4}{9} & for \quad i = 1...4 \\ \frac{1}{36} & for \quad i = 5...8 \end{cases} \quad (5)$$

Where α and c represent, respectively, the thermal diffusivity of the medium and the lattice velocity. The temperature is obtained after summing f_i over all directions:

$$T(\vec{r},t) = \sum_{i=0}^{n_v} f_i(\vec{r},t) \quad (6)$$

The equilibrium function $f_i^{eq}(\vec{r},t)$ is *given* by:

$$f_i^{eq}(\vec{r},t) = \omega_i T(\vec{r},t) \quad (7)$$

3. Discretization

The domain of interest is first divided into the desired number of triangular elements (Fig. 1a). The unknown distribution functions are stored in the grid nodes. As shown in figure 1b, non overlapping polygonal control volumes are constructed around each node of the grid by joining the centroid G_j of each triangular element with the midpoints M_1 and M_2 of the corresponding sides (Fig. 1c). The control volume, ΔV_N (Fig. 1b), is constructed by summing all sub volumes $\Delta V_{N,j}$ (Fig. 1c).

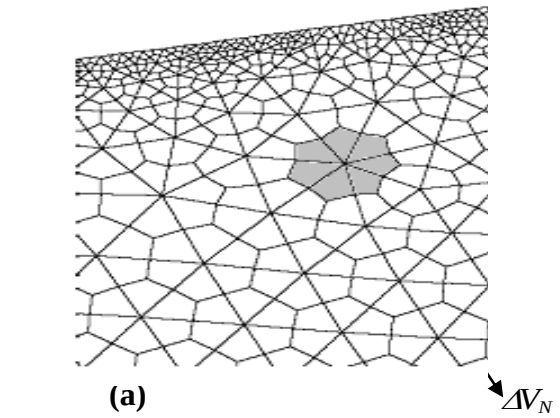

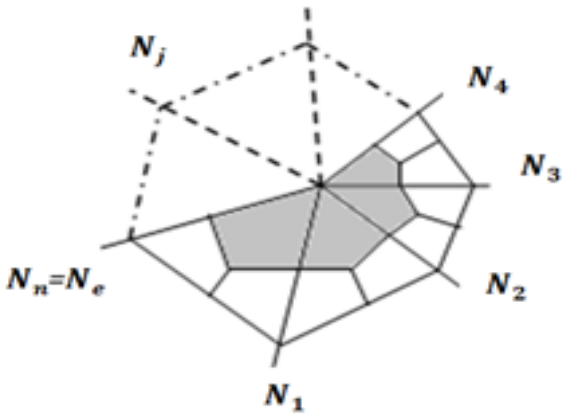

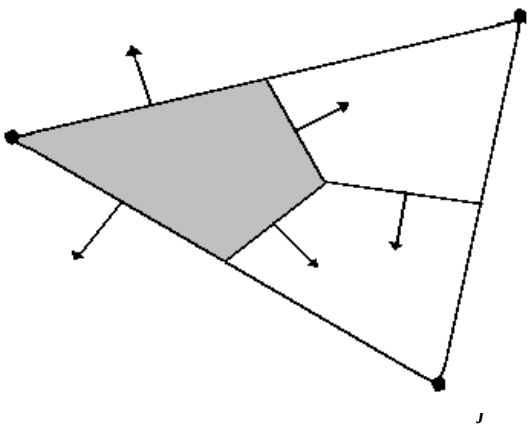

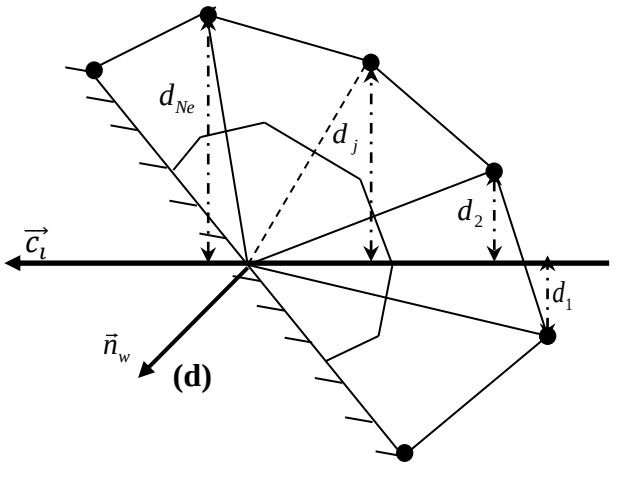

Figure 1: Spatial control volume: (a) unstructured mesh and polygonal control volume, (b) internal control volume, (c) triangular element, (d) orthogonal distance for Boltzmann equation

The computer code implementing the above method was written in Fortran 90 (F90). The unstructured mesh requires the connectivity information to be stated explicitly. In the current work, the connectivity information is conveniently handled using data structures and pointers in F90 language.

A ‘‘Control-Volume’’ data structure is employed in the present work on account of its suitability for control-volume finite-element technique. In this structure, we associate, particularly, to each node of the calculation domain, a number *N*, two coordinates x_N and y_N, and a number m_N which denotes its location (m_N is equal to zero if the node is inside the calculation domain and different from zero if it is on a boundary).

In order to derive the discretized form, Eq. 2 is integrated over the control volume ΔV_N and over the interval of time *[t; t +⊿t]*.

$$\underbrace{\int_{\Delta V_N}\int_{\Delta t}\frac{\partial f_i}{\partial t}dtdV}_{Q_1}+\underbrace{\int_{\Delta V_N}\int_{\Delta t}\vec{\nabla}.\left(\vec{c}_i f_i\right)dtdV}_{Q_2}=\underbrace{\int_{\Delta V_N}\int_{\Delta t}\left(\frac{f_i^{eq}-f_i}{\tau}\right)dtdV}_{Q_3} \quad (8)$$

To calculate the integrals Q_1 and Q_3 of Eq.8, the distribution function f_i is evaluated at the centroïd of the control volume, ΔV_N , and it is assumed to prevail over it. Then, the two terms can be written as:

$$Q_1=\alpha_{i,N,1}f_{i,N}-\beta_{i,N,1} \quad (9)$$

$$Q_3=\beta_{i,N,3}-\alpha_{i,N,3}f_{i,N} \quad (10)$$

Where $\alpha_{i,N,1}=\Delta V_N$, $\beta_{i,N,1}=\Delta V_N f_{i,N}^0$, $\alpha_{i,N,3}=\frac{\Delta t\Delta V_N}{\tau}$ and $\beta_{i,N,3}=\frac{\Delta t\Delta V_N}{\tau}f_{i,N}^{eq}$

In order to calculate the integral Q_2 of the Boltzmann equation, we have expressed it as follows:

$$Q_2=\int_{\Delta t}\sum_{j=1}^{N_e}\int_{\Delta V_{N,j}}\vec{\nabla}.\left(\vec{c}_i f_{i,j}\right)dtdV \quad (11)$$

Where N_e represents the total number of triangular elements surrounding the node *N*.

The divergence theorem permits us to express the term Q_2 as

$$Q_2=\Delta t\sum_{j=1}^{N_e}\int_{A_{N,j}}\vec{c}_i f_{i,j}\overrightarrow{dA} \quad (12)$$

The development of Eq.12 gives:

$$Q_2=\Delta t\sum_{j=1}^{N_e}\sum_{k=1}^{4}\int_{A_{N,j,k}}\vec{c}_i f_{i,j,k}\vec{n}_{j,k}dA \quad (13)$$

Where $f_{i,j,k}$ is the distribution function at the midpoint of the panel $A_{N,j,k}$ and $\vec{n}_{j,k}$ is the unit normal vector to the panel $A_{N,j,k}$ of the triangular element number j (Fig.1c).

And $A_{N,j,1}=M_1G_j$, $A_{N,j,2}=G_jM_2$, $A_{N,j,3}=M_2N$, $A_{N,j,4}=NM_1$

To approximate the integral of the distribution function $f_{i,j,k}$ over each panel $A_{N,j,k}$, the

distribution function is evaluated at the midpoint of the corresponding panel and it is assumed to prevail over it. Then Eq. (13) becomes:

$$Q_2=\Delta t\sum_{j=1}^{N_e}\sum_{k=1}^{4}G_{j,k}^i f_{i,j,k} \quad (14)$$

Where $G_{j,k}^i$ represents the directional weight associated to the triangular element number *j* at panel $A_{N,j,k}$ and is given by:

$$G_{j,k}^i=\int_{A_{j,k}}\vec{c}_i\vec{n}_{j,k}dA \quad (15)$$

We can note that, for any node N (a boundary node or an internal node), $G^i_{j,3} = -G^i_{j+1,4}$ $(j = 1,..., N_e - 1)$ and, if the location number m_N is equal to zero (the node N is inside the domain), $G^i_{N_e,3} = -G^i_{1,4}$. So, Eq. (14) can be written as:

$$Q_2 = \Delta t \sum_{j=1}^{N_e} \sum_{k=1}^{2} G^i_{j,k} f_{i,j,k} + Q_{2,b} \quad (16)$$

Where

$$Q_{2,b} = \begin{cases} \Delta t \left(G^i_{1,4} f_{i,1,4} + G^i_{N_e,3} f_{i,N_e,3} \right) & if \quad m_N \neq 0 \\ 0 & if \quad not \end{cases} \quad (17)$$

To obtain the desired expression of Q_2 , the distribution functions $f_{i,j,k}$ should be expressed in terms of nodal values of distribution functions.

The SPCU scheme (Skew Positive Coefficient Upwind) [22] is used to approximate the distribution functions $f_{i,j,1}$ and $f_{i,j,2}$ which appear in equation (16), in terms of nodal values of distribution functions. For example, the value of the distribution function $f_{i,j,1}$ on panel $A_{N,j,1}$ is expressed as:

$$f_{i,j,1} = g^{i+}_{j,1} f_{i,j,2} + \left(1 - g^{i+}_{j,1}\right) f_{i,N} \qquad if \quad G^i_{j,1} > 0 \quad (18)$$

$$f_{i,j,1} = g^{i-}_{j,1} f_{i,j,5} + \left(1 - g^{i-}_{j,1}\right) f_{i,N_j} \qquad if \quad G^i_{j,1} < 0 \quad (19)$$

Where

$$g^{i+}_{j,1} = Min\left(Max\left(-\frac{G^i_{j,2}}{G^i_{j,1}}, 0 \right), 1 \right) \quad (20)$$

$$g^{i-}_{j,1} = Min\left(Max\left(-\frac{G^i_{j,5}}{G^i_{j,1}}, 0 \right), 1 \right) \quad (21)$$

Using the following functions,

$$W^i_{j,k} = Max\left(\frac{G^i_{j,k}}{\left| G^i_{j,k} \right|}, 0 \right) \qquad k = 1,5 \quad (22)$$

the distribution functions $f_{i,j,1}$ and $f_{i,j,2}$ and $f_{i,j,5}$ can be written in the following forms:

$$f_{i,j,1} = W^i_{j,1} \left[g^{i+}_{j,1} f_{i,j,2} + \left(1 - g^{i+}_{j,1}\right) f_{i,N} \right] + \left(1 - W^i_{j,1}\right) \left[g^{i-}_{j,1} f_{i,j,5} + \left(1 - g^{i-}_{j,1}\right) f_{i,N_j} \right] \quad (23)$$

$$f_{i,j,2} = W^i_{j,2} \left[g^{i+}_{j,2} f_{i,j,2} + \left(1 - g^{i+}_{j,2}\right) f_{i,N} \right] + \left(1 - W^i_{j,2}\right) \left[g^{i-}_{j,2} f_{i,j,5} + \left(1 - g^{i-}_{j,2}\right) f_{i,N_{j+1}} \right] \quad (24)$$

$$f_{i,j,5} = W^i_{j,5} \left[g^{i+}_{j,5} f_{i,j,2} + \left(1 - g^{i+}_{j,5}\right) f_{i,N_{j+1}} \right] + \left(1 - W^i_{j,5}\right) \left[g^{i-}_{j,5} f_{i,j,1} + \left(1 - g^{i-}_{j,5}\right) f_{i,N_j} \right] \quad (25)$$

Equations (23), (24) and (25) can be assembled and written as follows:

$$FP^{ji} = E^{ji} FN^{ji} \qquad j = 1,..., N_e \quad (26)$$

Where

$$FP^{ji} = \begin{bmatrix} f_{i,j,1} \\ f_{i,j,2} \\ f_{i,j,5} \end{bmatrix} \quad (27)$$

$$FN^{ji} = \begin{bmatrix} f_{i,N} \\ f_{i,N_j} \\ f_{i,N_{j+1}} \end{bmatrix} \quad (28)$$

$$E^{ji} = \left(C^{ji}\right)^{-1} B^{ji} \quad (29)$$

$$C^{ji} = \begin{bmatrix} 1 & -W_{j,1}^{i} g_{j,1}^{i+} & -\left(1-W_{j,1}^{i}\right) g_{j,1}^{i-} \\ -W_{j,2}^{i} g_{j,2}^{i+} & 1 & -\left(1-W_{j,2}^{i}\right) g_{j,2}^{i-} \\ -\left(1-W_{j,5}^{i}\right) g_{j,5}^{i-} & -W_{j,5}^{i} g_{j,5}^{i+} & 1 \end{bmatrix} \quad (30)$$

$$B^{ji} = \begin{bmatrix} W_{j,1}^{i}\left(1-g_{j,1}^{i+}\right) & \left(1-W_{j,1}^{i}\right)\left(1-g_{j,1}^{i-}\right) & 0 \\ W_{j,2}^{i}\left(1-g_{j,2}^{i+}\right) & 0 & \left(1-W_{j,2}^{i}\right)\left(1-g_{j,2}^{i-}\right) \\ 0 & \left(1-W_{j,5}^{i}\right)\left(1-g_{j,5}^{i-}\right) & W_{j,5}^{i}\left(1-g_{j,5}^{i+}\right) \end{bmatrix} \quad (31)$$

Referring to Eq. (26), the distribution function $f_{i,j,k}$ ($k=1, 2$) can be expressed as:

$$f_{i,j,k} = E_{k1}^{ji} f_{i,N} + E_{k2}^{ji} f_{i,N_j} + E_{k3}^{ji} f_{i,N_{j+1}} \quad (32)$$

Using the number of nodes, N_n, neighboring the node N ($N_n=N_e$ if the node is inside the calculation domain) and replacing the distribution functions $f_{i,j,k}$ ($k=1, 2$ for a node interior the domain) which appear in Eq. (16) by their expressions [Eq. (32)], we obtain

$$Q_2 = \alpha_{i,N,2} f_{i,N} + \sum_{j=1}^{N_n} \gamma_{i,N_j} f_{i,N_j} - \beta_{i,N,2} \quad (33)$$

Where

$$\begin{cases} \alpha_{i,N,2} = \Delta t \sum_{j=1}^{N_n} \sum_{k=1}^{2} G_{j,k}^{i} E_{k1}^{ji} \\ \gamma_{i,N_j} = \Delta t \sum_{j=2}^{N_n} \sum_{k=1}^{2} G_{j,k}^{i} E_{k2}^{ji} + G_{j-1,k}^{i} E_{k3}^{j-1i} \;; \quad j = 2...N_n \\ \gamma_{i,N_1} = \Delta t \left(G_{1,k}^{i} E_{k2}^{1i} + G_{N_e,k}^{i} E_{k3}^{N_e i} \right) ; j=1 \\ \beta_{i,N,2} = -Q_{2,b} \end{cases}$$

Replacing the quantities Q_1, Q_2 and Q_3 which appear in Eq. (8) by their expressions [Eqs. (9), (10) and (33)], the algebraic system of the discretized Boltzmann equation can be written in the following form:

$$\alpha_{i,N} f_{i,N} + \sum_{j=1}^{N_n} \gamma_{i,N_j} f_{i,N_j} = \beta_{i,N} \quad (34)$$

Where

$$\alpha_{i,N} = \alpha_{i,N,1} + \alpha_{i,N,2} + \alpha_{i,N,3} \quad (35)$$

$$\beta_{i,N} = \beta_{i,N,1} + \beta_{i,N,2} + \beta_{i,N,3} \quad (36)$$

In the present study, the energy equation is subjected to Dirichlet boundary condition. To express this condition the bounce-back concept in the LBM [21] was used for the unknown incoming distribution functions ($\vec{c}_i.\vec{n}_j < 0$) and the modified STEP scheme was applied to the unknown outgoing distribution functions ($\vec{c}_i.\vec{n}_j > 0$).

For $\vec{c}_i.\vec{n}_{j,k} < 0$, the bounce-back scheme permits us to write

$$f_{i,N} + f_{i',N} = 2\omega_i T_N^0 \quad (37)$$

By identification, we obtain

$$\alpha_{i,N} = 1,\ CL_{i,N}^{i'} = 1,\ \gamma_{i,N_j} = 0 \text{ and } \beta_{i,N} = 2\omega_i T_N^0 \quad (38)$$

For $\vec{c}_i.\vec{n}_{j,k} > 0$, the following interpolation scheme is proposed.

$$f_{i,N} = \sum_{j=1}^{N_e} \frac{S - d_j}{(N_e - 1)S} f_{i,N_j} \quad (39)$$

Where

$$S = \sum_{j=1}^{N_e} d_j \quad (40)$$

d_j represents the orthogonal distance measured from the node *N* to line $(N, \vec{c}_i)$ (Fig. 1d).

Then

$$f_{i,N} = \sum_{j=1}^{N_e} \frac{S - d_j}{(N_e - 1)S} \left(\frac{\tau}{\tau + \Delta t} f^0_{i,N_j} + \frac{\Delta t}{\tau + \Delta t} f^{eq}_{i,N_j} \right) \quad (41)$$

$$\alpha_{i,N} = 1,\ CL^{i'}_{i,N} = 0,\ \gamma_{i,N_j} = 0 \text{ and } \beta_{i,N} = \sum_{j=1}^{N_e} \frac{S - d_j}{(N_e - 1)S} \left(\frac{\tau}{\tau + \Delta t} f^0_{i,N_j} + \frac{\Delta t}{\tau + \Delta t} f^{eq}_{i,N_j} \right) \quad (42)$$

Adopting these schemes, the Boltzmann equation on the boundary is expressed as:

$$\alpha_{i,N} f_{i,N} + \sum_{j=1}^{N_n} \gamma_{i,N_j} f_{i,N_j} + CL^{i'}_{i,N} f_{i',N} = \beta_{i,N} \quad (43)$$

It is very important to indicate that the terms $\alpha_{i,N}$, γ_{i,N_j}, $CL^{i'}_{i',N}$ and $\beta_{i,N}$ in Eq. (43) depend only on physical properties, geometric coefficients, and temperature. Thus, the obtained algebraic system is linear. It can be solved by a direct or an iterative method in which all the distribution functions ($f_{i,N}$) are calculated simultaneously after each iteration. For these two methods (direct or iterative), formulation of a matrix system is necessary.

4. Different schemes for time-discretization

For the discretization, explicit scheme can be used. In this case Eq.43 becomes:

$$f_{i,N} = \frac{\beta_{i,N} - \sum_{j=1}^{N_n} \gamma_{i,N_j} f^0_{i,N_j} - (\alpha_{i,N,2} + \alpha_{i,N,3}) f^0_{i,N} - CL^{i'}_{i,N} f^0_{i',N}}{\alpha_{i,N,1}} \quad (44)$$

In the present work, the authors propose a new scheme for the time discretization. For this scheme, the distribution function, f_i, at the calculation node number *N* is considered at time $t+\Delta t$ for the three terms of Eq.8. For the nodes neighboring the calculation node *N*, the distribution function, f_i is taken at time *t*. Using this scheme, the different terms of Eq.8 can be written as:

$$Q_1 = \alpha_{i,N,1} f_{i,N} - \beta_{i,N,1} \quad (45)$$

$$Q_2 = \alpha_{i,N,2} f_{i,N} + \sum_{j=1}^{N_n} \gamma_{i,N_j} f^0_{i,N_j} - \beta_{i,N,2} \quad (46)$$

$$Q_3 = \beta_{i,N,3} - \alpha_{i,N,3} f_{i,N} \quad (47)$$

In these conditions, Eq.8 takes the following form:

$$f_{i,N} = \frac{\beta_{i,N} - \sum_{j=1}^{N_n} \gamma_{i,N_j} f^0_{i,N_j} - CL^{i'}_{i,N} f^0_{i',N}}{\alpha_{i,N}} \quad (48)$$

5. Matrix formulation

To formulate the matrix system of the discretized equations [Eq. (43)], the distribution function $f_{i,N}$, on the node denoted by the number *N* and in the direction i, will be represented by $F(l)$, where *l* is expressed in terms of *N* and *i* as follows:

$$l = (N-1)n_v + i \quad (49)$$

Using this definition of the distribution function vector *F*, the algebraic system that contains $N_t \times n_v$ equations can be written in the following matrix form:

$$AF = b \quad (50)$$

Each line denoted by *l* (*l=1,…,Nt*n*$_v$) of the matrix *A* contains the coefficients of the discretized form of the LBE (Eq.50) established at the node of the grid number *N* and the direction *i*. Using this definition, the coefficients of the matrix *A* can be written as

$$A_{lk} = \begin{cases} \alpha_{i,N} \quad for \quad \begin{cases} i = 1...n_v \\ k = (N-1)n_v + i \\ l = (N-1)n_v + i \end{cases} \\ \gamma_{i,N_j} \quad for \quad \begin{cases} N_j = N_1 ... N_{Nn} \\ k = (N_j - 1)n_v + i \\ l = (N_j - 1)n_v + i \end{cases} \\ CL_{i,N}^{i'} \quad for \quad \begin{cases} i' = 1...n_v \\ k = (N-1)n_v + i' \\ l = (N-1)n_v + i \end{cases} \\ 0 \quad for\ the\ other\ values\ of\ l\ and\ k \end{cases} \quad (51)$$

$$b_l = \beta_{i,N} \quad (52)$$

The conditioned conjugate gradient squared method (CCGS), which is frequently used in computational fluid dynamics (CFD) problems, is used to solve the established matrix system of the discretized LBE.

6. Solution procedure

1- Calculate the geometric parameters (control volumes, surfaces,…).

2- Calculate the coefficients $CL_{i,N}^{i'}$ and γ_{i,N_j} .

3- Given the initial temperature field, compute f_i^{eq} (Eq.7) and then set $f_i = f_i^{eq}$.

4- Compute the coefficients $\alpha_{i,N}$ and $\beta_{i,N}$.

5- Compute the distribution functions $f_{i,N}^{*}$ (Eq.48).

6- Compute temperature field (Eq.6).

7- Calculate f_i^{eq}(Eq.7).

8- Terminate the process when the steady state is achieved. Else and go step 4.

7. Results and discussion

Following the theoretical and numerical analyses presented in the current study, a computer code has been developed and three test cases (a square enclosure, an equilateral triangular enclosure, and a quarter of a circle with rectangular enclosure) are investigated to examine the accuracy of the proposed unstructured CVLBM to predict unsteady conduction heat transfer in 2D- regular and complex geometries. To study the suitability of the proposed approach, the same problems are solved using the classical Control Volume Finite Element Method.

In both the CVLBM and the CVFEM, steady-state conditions were assumed to have been achieved when the temperature difference between two consecutive time levels at each node did not exceed 1×10^{-6}. Non-dimensional time was defined as $\xi=\alpha t/L^2$ where L is the characteristic length and in both the CVLBM and the CVFEM, $\Delta\xi$ was taken as 1×10^{-4}. It is to be noted that in solving heat conduction problems if the non-dimensional time is defined as $\xi=\alpha t/L^2$, the non-dimensional forms of Eq. (2) to be solved in the CVLBM and

Eq. (1) in the CVFEM, do not contain thermal diffusivity α term. In both the methods, α is embedded in the non-dimensional time ξ.

The first problem examined is a square enclosure which is depicted in figure 2. Initially, the system is assumed to be at a constant non-dimensional temperature $\theta_i=0.5$ ($\theta=T/T_{ref}$). For t>0, the wall 3 is maintained at $\theta_1=1.0$ and all the other walls (1, 2 and 4) are at $\theta_2=0.5$.

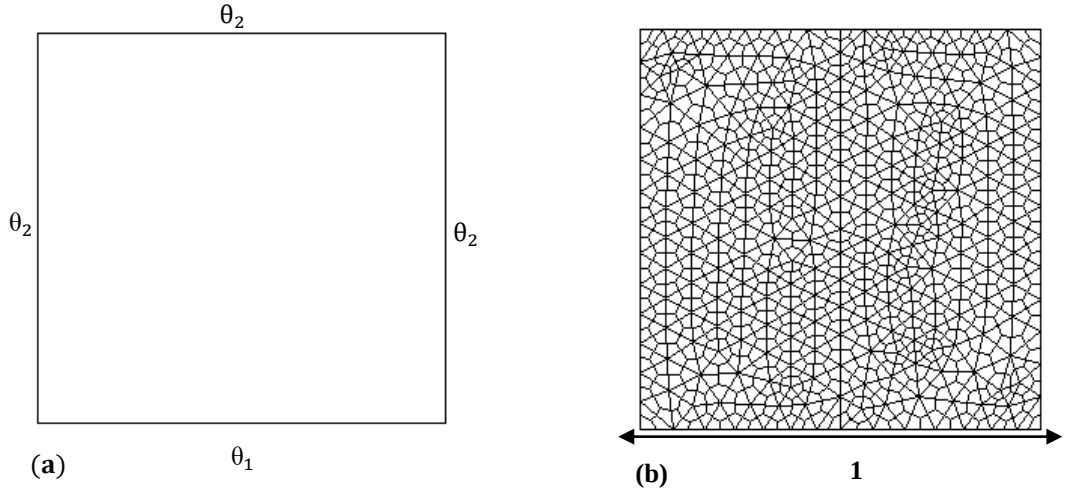

Figure 2: A square enclosure: (a) schematic diagram; (b) unstructured mesh

In order to check the computational efficiency of the three schemes for time-discretization (implicit scheme, proposed scheme and explicit scheme), different simulations are done and the obtained results are compared with CVFEM results (Fig. 3). For each scheme the time evolution of the average bed temperature and the corresponding CPU time are determined for different number of total nodes of the calculation domain. Table 1 lists the total number of nodes (or control volumes) which gives the best solution and the CPU time required by the different schemes to reach the steady state solution using an Intel (R) Core (TM) i3 CPU 2.13 computer.

It can be seen from figure 3 that the CVLBM with implicit scheme and the CVLBM with the proposed scheme compare very well with the CVFEM results. However, the results obtained by the explicit scheme present a large difference compared to the CVFEM results.

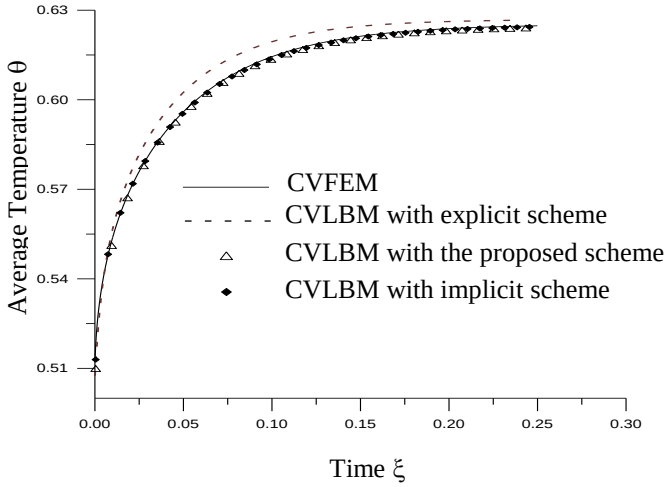

Figure 3: In a 2-D square enclosure at different instants, comparison of centerline (X=0.5) non-dimensional temperature.

Table 1: CPU time for the different time-discretization schemes

	N_t	CPU time *(s)*
Implicit scheme	1941	502.5
Proposed scheme	2553	43.5
Explicit scheme	5415	84.9

On the other hand, table 1 shows that the proposed scheme is very fast compared to the implicit scheme (about 10 times very fast) but needs more number of control volumes.

For the following results, the proposed scheme for time-discretization is used.

In Fig. 4, centerline (X=0.5) non-dimensional temperature has been compared at different instants ξ. It can be noticed that the CVLBM results are totally consistent with the standard CVFEM results

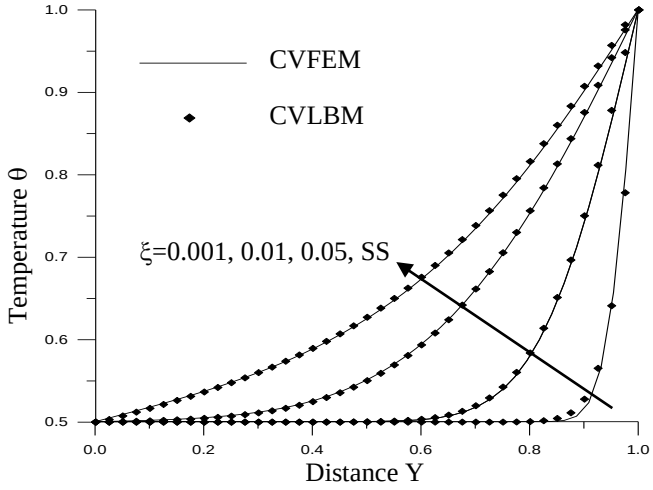

Figure 4: In a 2-D square enclosure at different instants, comparison of centerline (X=0.5) non-dimensional temperature

In Fig. 5, at different instants ξ, isotherms of the two methods have been compared. It can be seen from these figures that the CVLBM results compare very well with the CVFEM results

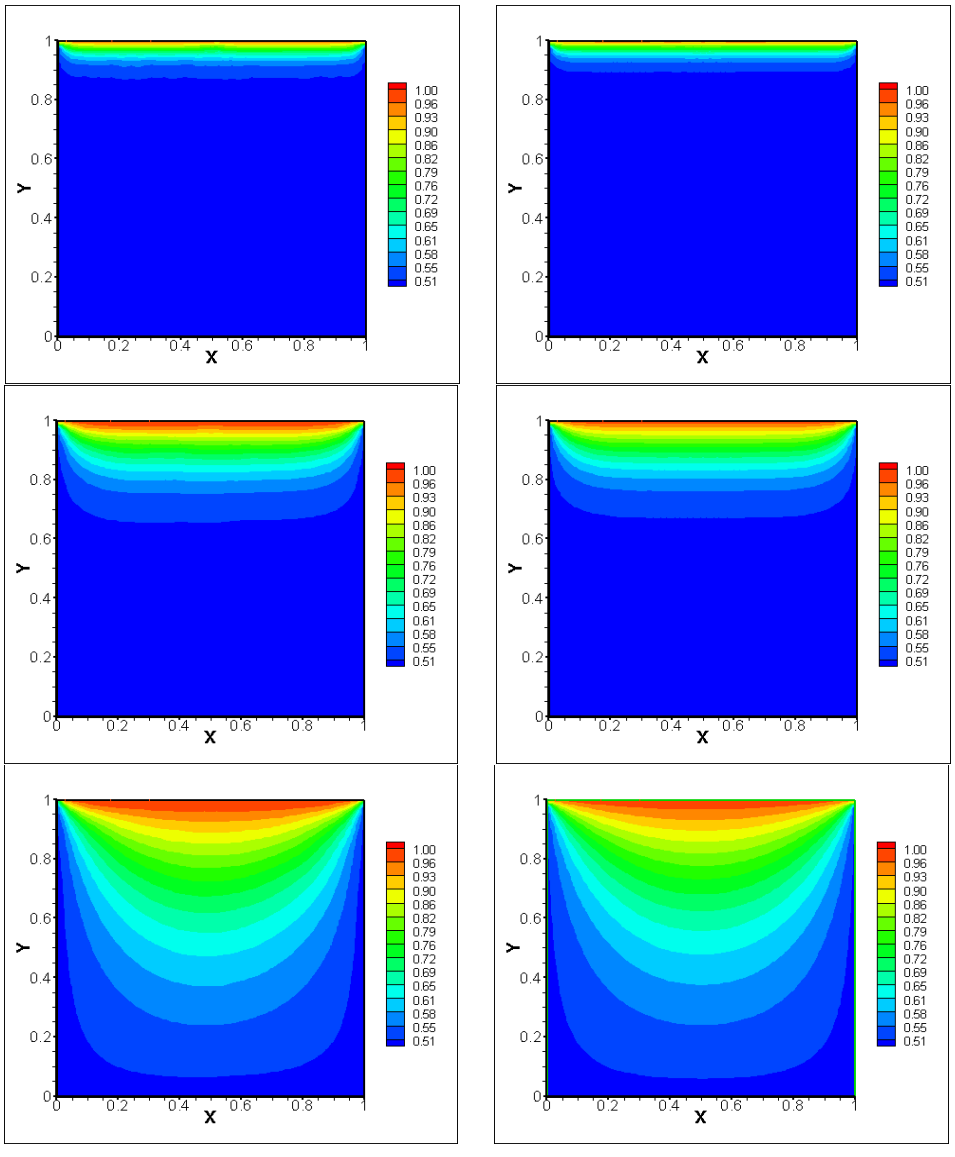

(a) (b)

Figure 5: In a 2-D square enclosure, time-space evolution of non-dimensional average temperature calculated by (a) CVLBM and (b) CVFEM.

In Fig. 6, the effect of the heat generation is shown. It can be seen that this effect is very slight in the beginning compared to the steady-state because it requires some time to influence the temperature profile.

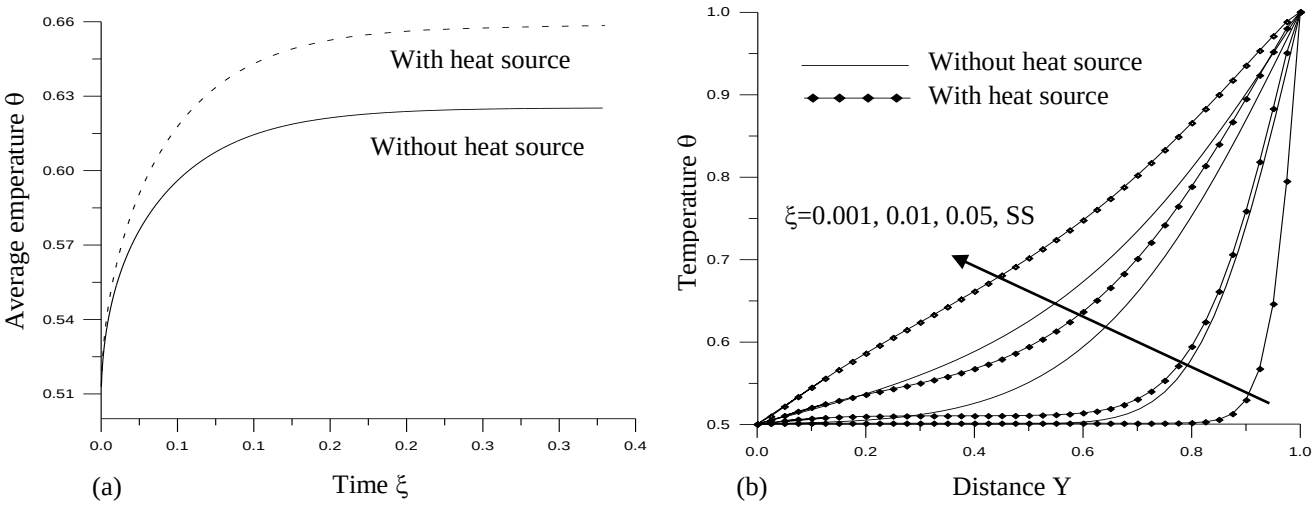

Figure 6: In a 2-D square enclosure, effect of heat generation on (a) average non-dimensional temperature and (b) on the centerline (x=0.5) non dimensional temperature.

Once we tested the accuracy of this new approach for a simple enclosure, we adopted it for the case of irregular geometries.

For the second test case, the CVLBM is applied to an equilateral triangular enclosure which is depicted in figure 8. Initially, the system is assumed to be at a constant non-dimensional temperature $\theta_i=0.5$. For t>0, All walls are maintained at $\theta_1=1.0$. For the equilateral triangular enclosure, 960 control volumes were used.

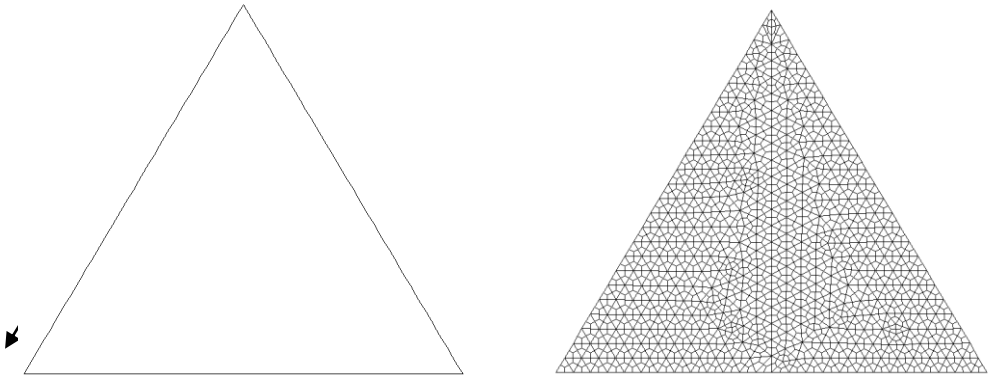

Figure 7: An equilateral triangular enclosure: (a) schematic diagram; (b) unstructured mesh.

The centerline (X=0.5) non-dimensional temperature (Fig.8) and the isotherms results (Fig. 9) have been compared at different instants ξ .

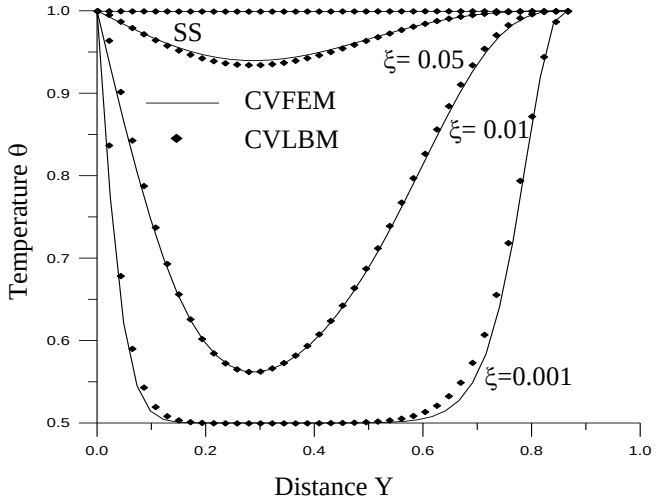

Figure 8: In a 2-D equilateral triangular enclosure, at different instants, comparison of centerline (X =0.5) non-dimensional temperature

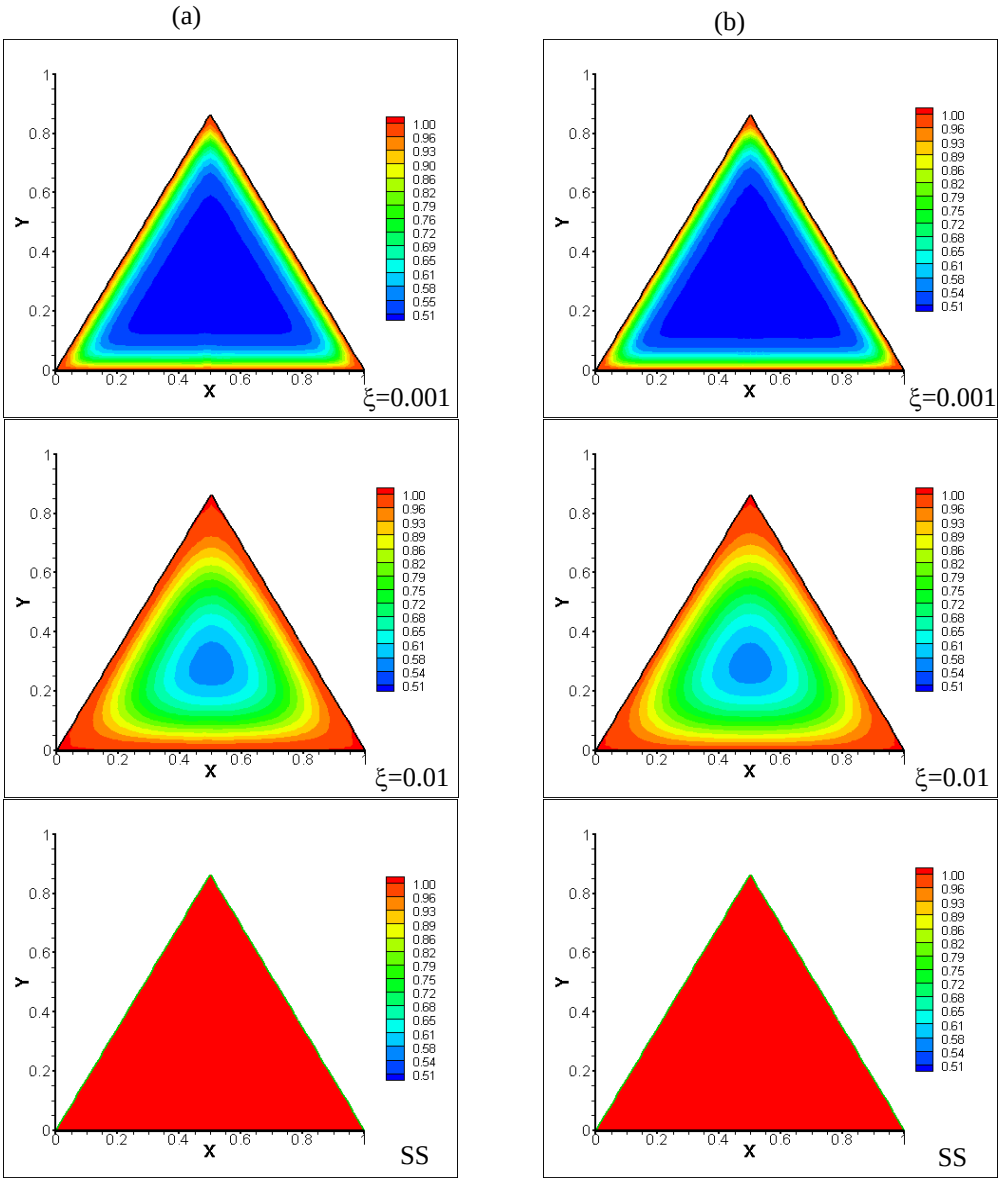

Figure 9: In a 2-D equilateral triangular enclosure, time-space evolution of non-dimensional temperature calculated by (a) the CVLBM and (b) the CVFEM.

For the last problem, a quarter of a circle with a rectangular region added to the top as shown in Figure 10 is chosen. Initially, the system is assumed to be at $\theta_i=0.5$. For t>0, the wall-1 is maintained at $\theta_1=1.0$ and all the other walls (2, 3 and 4) are at $\theta=0.5$. In the CVLBM and the CVFEM, 2790 control volumes were used.

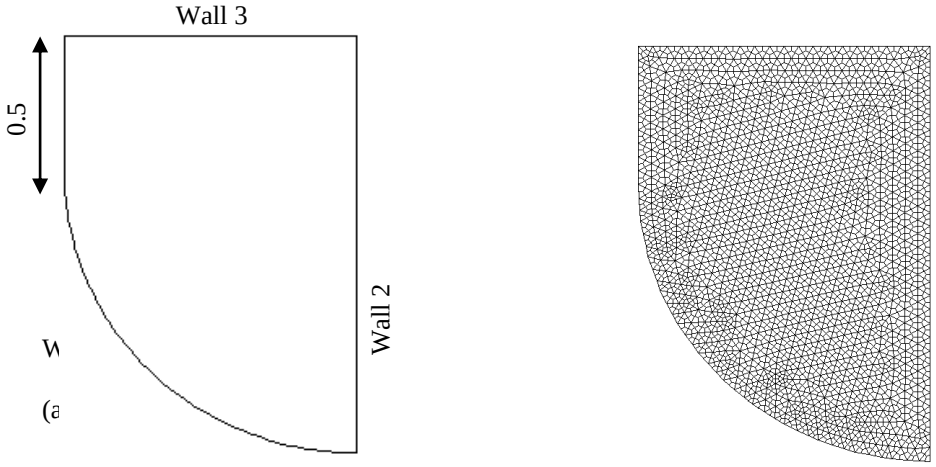

Figure 10: A quarter of a circle with rectangular enclosure: (a) schematic diagram, (b) unstructured mesh.

The non-dimensional temperature profile along the line CD and the isotherms results at different instants ξ, given by the two numerical approaches are presented, respectively, in Figs.11 and 12.
It all the cases, it can be noticed that the CVLBM results compare very well with the CVFEM results.

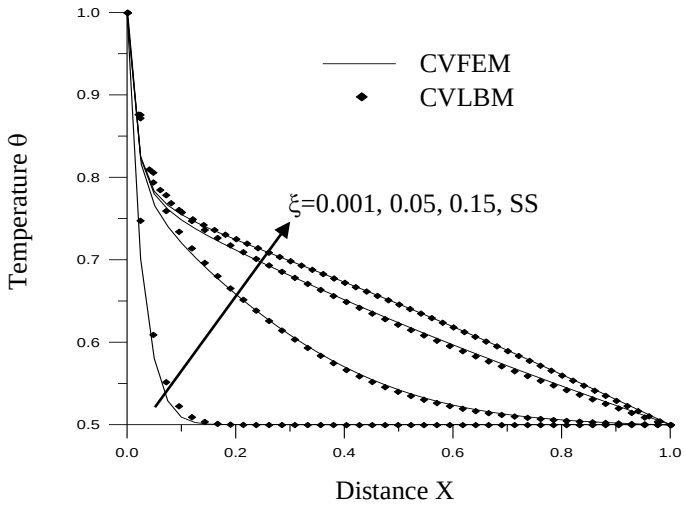

Figure 11: In a 2-D quarter of a circle with rectangular square enclosure: comparison of non-dimensional temperature at line CD at different instants.

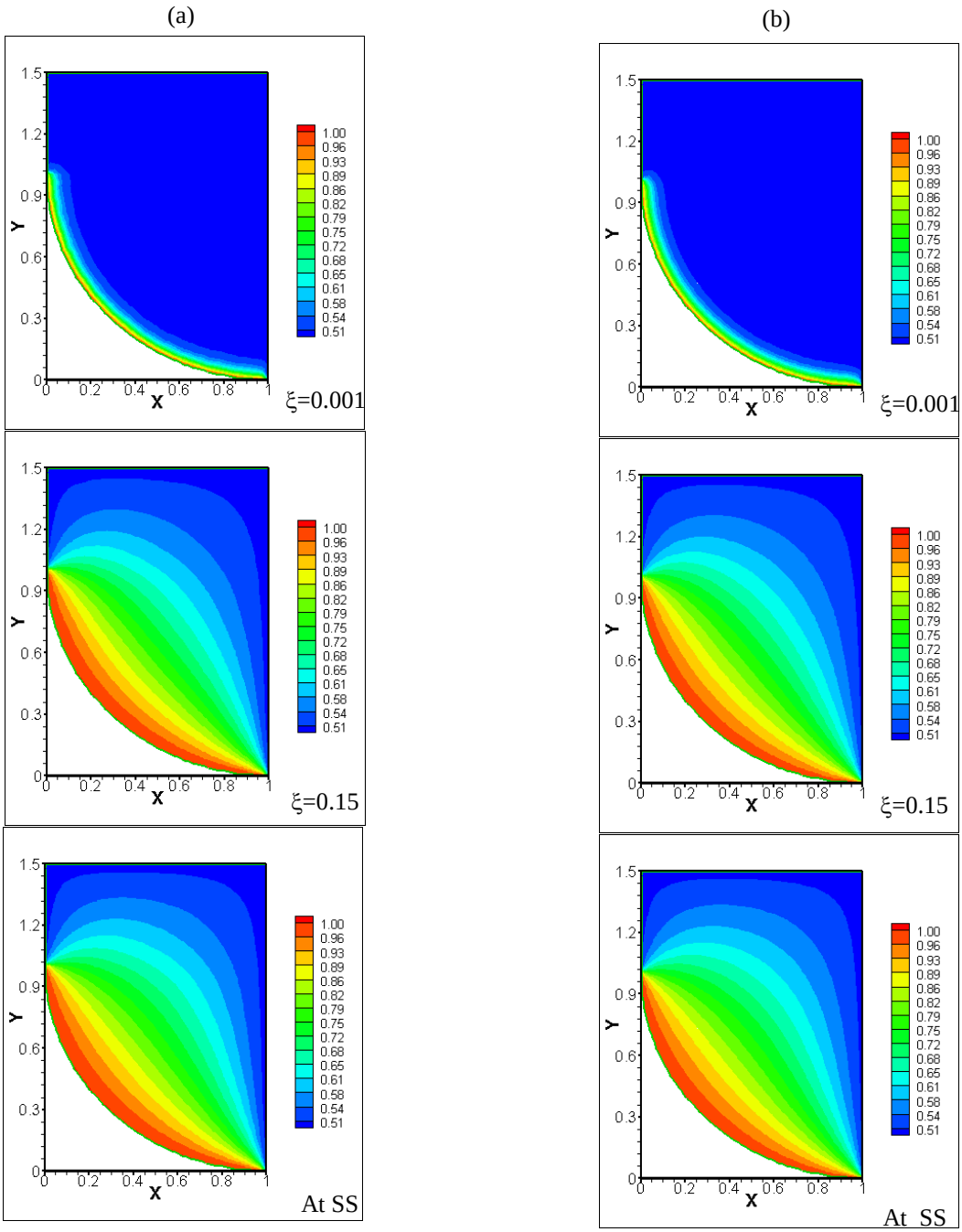

Figure 12: In a 2-D quarter of a circle with rectangular square enclosure: Time-space evolution of non-dimensional temperature calculated by (a) the CVLBM and (b) the CVFEM.

8. Conclusion

In this study an unstructured Control-Volume-Lattice Boltzmann Method (CVLBM) has been developed for the numerical prediction of 2D-unsteady conduction heat transfer in realistic applications with complex enclosures. This method shares the same grid generation strategy and the same basic philosophy of the CVFEM used in computational fluid dynamics. The steps of establishment and the final form of the general discretization equation were derived here using the SPCU scheme. The proposed method was applied to such diverse examples as a square enclosure, an equilateral triangular enclosure, and a quarter of a circle with a rectangular enclosure. In addition, a new time-discretization scheme was proposed and compared with implicit and explicit schemes. The obtained results show that the presented numerical method is flexible in treating unsteady heat conduction within complex geometry and stable. On the other hand, the computer procedure based on the proposed time-discretization scheme gives reasonable results and it is very fast compared to the implicit scheme.

REFERENCES

[1] K. Hejranfar, E. Ezzatneshan, Implementation of a high-order compact finite-difference lattice Boltzmann method in generalized curvilinear coordinates, Comput. Phys, volume 267, pages 28–49, 2014.
[2] M. B. Reider, J. D. Sterling, Accuracy of discrete velocity BGK models for the simulation of the incompressible Navier–Stokes equations, Comput. Fluids, volume 24, pages 459–467, 1995.
[3] R. Mei, W. Shyy, On the finite difference-based lattice Boltzmann method in curvilinear coordinates, Comput. Phys, volume 143, pages 426–448, 1998.
[4] J. Tolke, M. Krafczyk, M. Schulz, E. Rank, Implicit discretization and non uniform refinement approaches for FD discretizations of LBGK models, Modern Phys. Volume 9, pages 1143–1157, 1998.
[5] Z. Guo, T.S. Zhao, Explicit finite-difference lattice Boltzmann method for curvilinear coordinates, Phys. Rev, volume 67, 2003.
[6] V. Sofonea, R. F. Sekerka,Viscosity of finite difference lattice Boltzmann models, Comput. Phys, volume 184, pages 422–434, 2003.
[7] Fatih çevik, Göktan Güzel, Badri Yagiz, M.Haluk Aksel, Kahraman Albayrak, Finite- difference implementation of Lattice Boltzmann Method for use with non-uniform grids, Ankara International Aerospace Conference, volume 143, 2013.
[8] H. Chen, Volumetric formulation of the lattice Boltzmann method for fluid dynamics: basic concept, Phys. Rev. E58 (1998) 3955–3963.
[9] G. Peng, H. Xi, C. Duncan, S. H. Chou, Finite Volume scheme for the Lattice Boltzmann Method on unstructured meshes, Phys. Rev, volume 59, 1999.
[10] H. Xi, G. Peng, S.-H. Chou, Finite Volume Lattice Boltzmann method, Phys. Rev, volume 59, 1999.
[11] S. Ubertini, G. Bella, S. Succi, Unstructured lattice Boltzmann method: further development, Phys. Rev, volume 68, 2003.
[12] M. Stiebler, J. Tolke, M. Krafczyk, An upwind discretization scheme for the finite volume lattice Boltzmann method, Comput. Fluids, volume 35, pages 814–819, 2006.
[13] F. Dubois, P. Lallemand, On lattice Boltzmann scheme, finite volumes and boundary conditions, Prog. Comput. Fluid Dyn, volume 8, pages 11–24, 2008.
[14] D.V. Patil, K. N. Lakshmisha, Finite volume TVD formulation of lattice Boltzmann simulation on unstructured mesh, Comput. Phys, volume 228, pages, 5262–5279, 2009.
[15] Y. Li, E.J. Le Boeuf, P.K. Basu, Least-squares finite-element scheme for the lattice Boltzmann method on an unstructured mesh, Phys. Rev, volume 72, 2005.
[16] X. Shi, J. Lin, Z.Yu, Discontinuous Galerkin spectral element lattice Boltzmann method on triangular element, Numer. Methods Fluids, volume 42, pages 1249–1261, 2003.
[17] M. Min, T. Lee, A spectral-element discontinuous Galerkin lattice Boltzmann method for nearly incompressible flows, Comput. Phys, volume 230, pages 245–259, 2011.
[18] S. C. Mishra, B.Mondal and T.Kush, Solving transient heat conduction problems on uniform and non-uniform lattices using the lattice Boltzmann method, International Communications in Heat and Mass transfer, volume 36, pages 322-328, 2009.
[19] B. Mondal, X. Li, Effect of volumetric radiation on natural convection in a square cavity using lattice Boltzmann method with non-uniform lattices, Int. J. Heat Mass Transfer, volume 53, pages 4935–4948, 2010.
[20] Zi- Xiang Tong, Ya- Ling He, Wei- Wei Yang, Wen- Qan Tao, A coupling scheme of Lattice Boltzmann Method and Finite Volume Method for multi-component diffusion processes, Proceedings of the 15th international heat transfer conference, Japan, 2014.
[21] S. C. Mishra, A. Lankadasu, K.N. Beronov, Application of the lattice Boltzmann method for solving the energy equation of a 2-D transient conduction– radiation problem, International Journal of Heat and Mass Transfer, volume 48, pages 3648–3659, 2005.
[22] D.R. Rousse, G. Gautier and J. F. Sacadura, Une fonction d'interpolation produisant des coefficients positifs pour le rayonnement, Congrès français de thermique, Lyon, France, 2000.